Electronic Supplementary Material (ESI) for Faraday Discussions.

Supporting Information for: Exploring the Selectivity of Cytochrome P450 for Enhanced Novel Anticancer Agent Synthesis

Janko Čivić [a], Neil R. McFarlane [a], Joleen Masschelein [b], Jeremy N. Harvey [a]

[a] Janko Čivić, Neil R. McFarlane, Prof. Jeremy N. Harvey
Department of Chemistry
KU Leuven
B-3001 Leuven Celestijnenlaan 200f- box 2404, Belgium
E-Mail: janko.civic@kuleuven.be
E-Mail: neilrory.mcfarlane@kuleuven.be
E-Mail: jeremy.harvey@kuleuven.be

[b] Joleen Masschelein
Department of Biology
KU Leuven
B-3001 Leuven Kasteelpark Arenberg 31 - box 2438, Belgium
E-Mail: joleen.masschelein@kuleuven.be

Table S1: *Summary of BLAST sequence alignment results against the sequence of OxiK with the Protein Data Bank, where the first row contains the relevant data for OxiK. In order, the columns are the organism where the sequence comes from, the UniProt accession code, the Protein Data Bank accession code, the BLAST score calculated against OxiK, the percentage identity as compared to OxiK, the RMSD of the Protein Data Bank 3D structure against AlphaFold entry A0A2N0DV48 as calculated in PyMOL, whether the structure is apo or holo, any additional notes, and the relevant reference.*

Organism	UniProt Code	pdb id	BLAST Score	Per. Identity	RMSD (Å)	Apo/Holo	Notes	Reference
(*OxiK*) Pseudomonas baetica	A0A2N0DV48	-	-	-	-	Apo	-	-
Streptomyces avermitilis	Q82D73	7WZL	85.9	24.263	1.857	Apo	-	[1]
Deinococcus aerius	A0A2I9DQ46	7F3H	75.9	22.65	1.742	Apo	-	[2]
Priestia megaterium	P14779	7WG0	75.9	21.649	2.645	Holo	Complex with N-palmitoyl-L-phenylalanine bound, Manganese Protoporphyrin IX-Reconstituted	[3]
Priestia megaterium	P14779	4RSN	74.7	22.099	2.995	Apo	E267V mutant	[4]
Priestia megaterium	P14779	3HF2	74.3	22.099	1.807	Apo	I401P mutant	[5]
Deinococcus apachensis	N/R	7F3W	71.6	22.436	1.695	Apo	N190F/V356L/A486E mutant	[6]
Arabidopsis thaliana	O64989	6A15	68.6	26.54	2.827	Holo	Complex with cholesterol	[7]
Arabidopsis thaliana	O64989	6A16	68.2	27.014	1.788	Holo	Complex with uniconazole	[7]
Arabidopsis thaliana	O64989	6A17	67.8	25.926	1.582	Holo	Complex with brassinazole	[7]
Peribacillus butanolivorans	Q06069	5XNT	63.2	24.576	5.433	Apo	-	[8]
Priestia megaterium	Q06069	4YT3	62.8	25.07	4.946	Apo	-	[9]
Sorghum bicolor	Q94IP1	6VBY	60.1	23.11	3.067	Holo	Complex with cinnamic acid	[10]
Nocardia farcinica IFM 10152	Q5YNS8	4J6B	55.8	23.615	4.946	Holo	Complex with pregnenolone	[11]
Nocardia farcinica IFM 10152	Q5YNS8	6TO2	55.8	23.615	5.433	Holo	Complex with 5alpha-Androstan-3-one	[12]
Priestia megaterium DSM 319	D5DF88	5OFQ	51.6	23.227	3.067	Apo	-	[13]
Naegleria fowleri	A0A2H4A2U9	6AY6	49.7	21.591	3.701	Holo	Complex with voriconazole	[14]
Bacillus sp. (in: firmicutes)	E5WPM6	8HG9	49.3	24.017	3.403	Apo	-	[15]
Naegleria fowleri	A0A2H4A2U9	6AY4	49.3	21.591	3.725	Holo	Complex with fluconazole	[14]
Naegleria fowleri	A0A2H4A2U9	5TL8	48.9	21.591	3.777	Holo	Complex with posaconazole	[16]
Medicago truncatula	A0A072UMR6	8E83	48.9	20.041	2.736	Apo	-	[17]
Streptomyces violaceoruber	A0A1V0UEC8	6A7J	45.4	26.263	3.006	Holo	Complex with testosterone	[18]
Bacillus subtilis subsp. subtilis str. 168	O31785	4YZR	43.9	24.312	7.533	Apo	Also from a polyketide synthase cluster	[19]
Streptomyces sp. JS01	A0A087KD84	6A7I	42.7	25.253	10.353	Apo	-	[18]
Priestia megaterium DSM 319	D5DF35	7Q9E	42.7	21.963	4.335	Apo	-	[20]

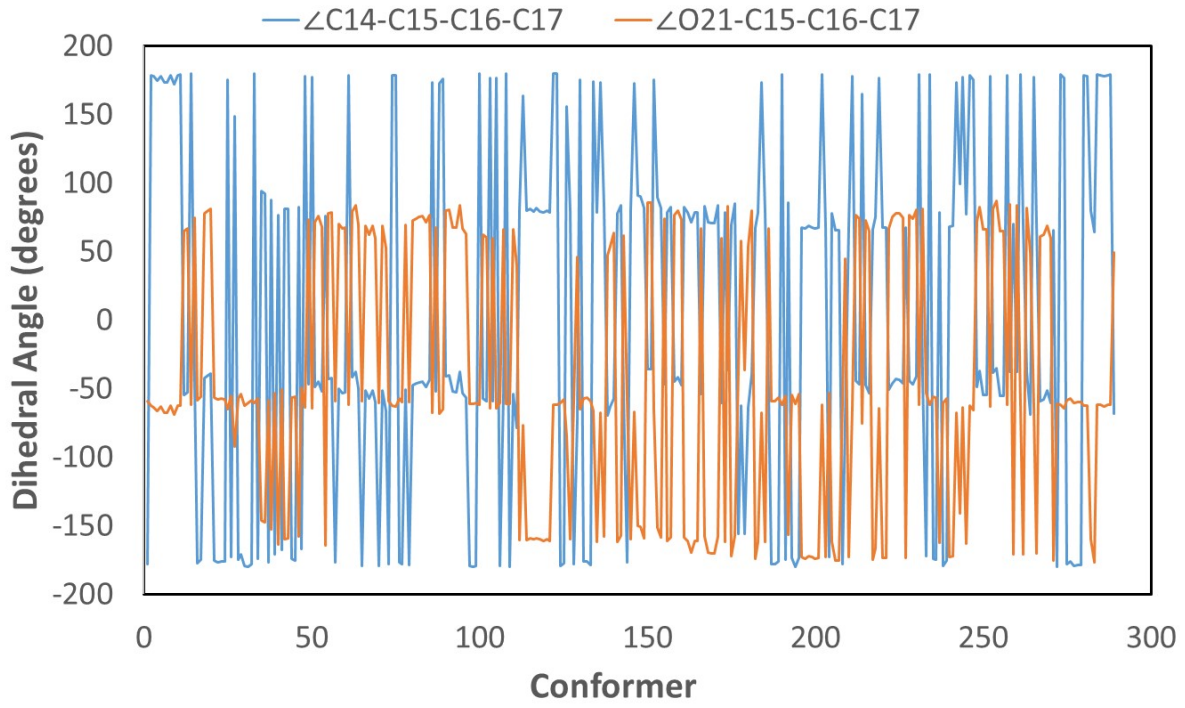

Figure S1: *Plot of two dihedral angles, ∠C14-C15-C16-C17 and ∠O21-C15-C16-C17, of all conformers found in the conformational search. Dihedral angles are given in degrees for easier interpretation.*

Run	Calculation type	Restraints (kcal/mol Å^2)	Constant	Minimization steps / Simulation time	Shake	Timestep (fs)
1	minimization (CPU)	non-solvent 200	V	10 000 steps	No	-
2	minimization (CPU)	-	V	10 000 steps	No	-
3	heating (CPU) 0-300 K	non-solvent 10	V	20 ps	Yes	2
4	pressure equilibration (CPU)	non-solvent 10	P	10 ps	Yes	2
5	pressure equilibration (GPU)	non-solvent 10	P	1 ns	Yes	2
6	equilibration (GPU)	substrate 5	V	1 ns	Yes	2
7	equilibration (GPU)	substrate 5	V	1 ns	Yes	2
8	equilibration (GPU)	-	V	1 ns	Yes	2
9	production (GPU)	-	V	100 ns	Yes	2

Table S2: *MD simulations protocol.*

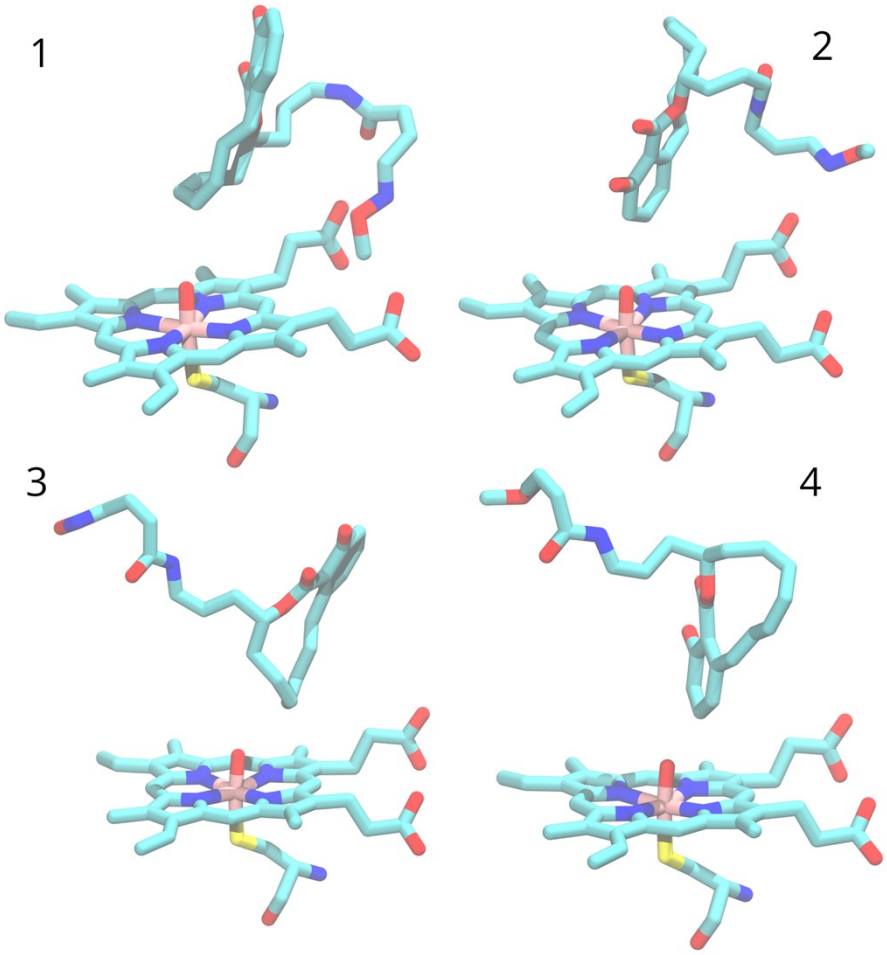

Figure S2: *Starting poses selected for molecular dynamics simulations. Colours: cyan, carbon; red, oxygen; blue, nitrogen; yellow, sulphur; pink, iron; white, hydrogen.*

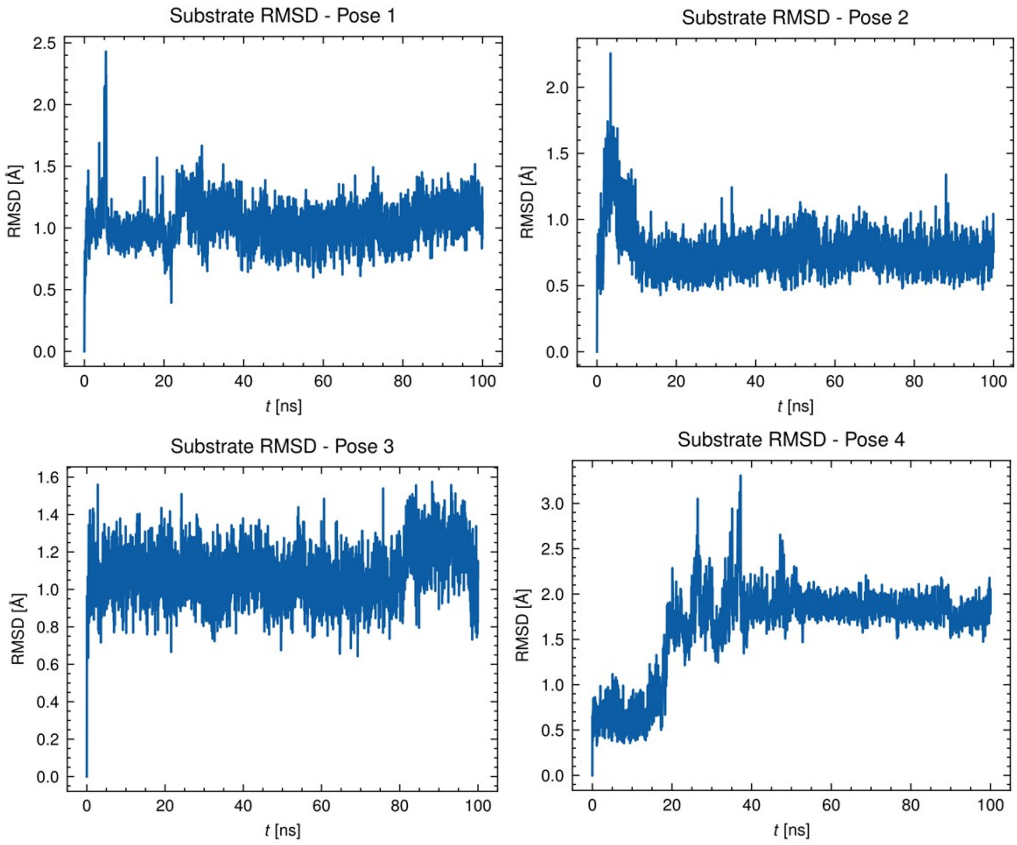

Figure S3: *RMSD of the oximidine substrate during the 100 ns MD simulations in different poses.*

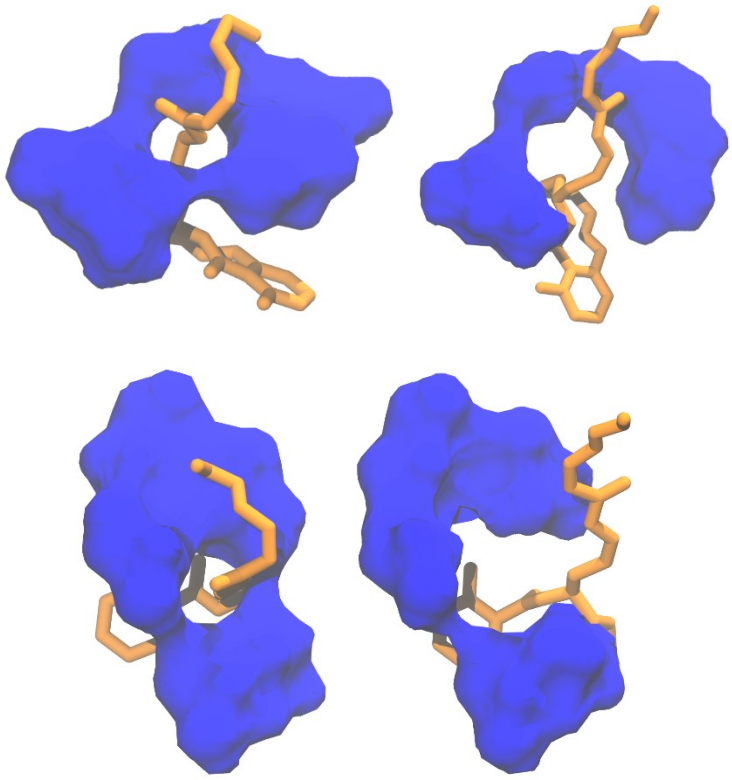

Figure S4: *Shape of the channel entrance after docking (left) and after MD simulations (right) of pose 3 (top) and pose 4 (bottom). The entrance forming residues Gly272, Leu268, Thr443, and Ser444 are shown as a blue surface. The substrate is represented as sticks in orange.*

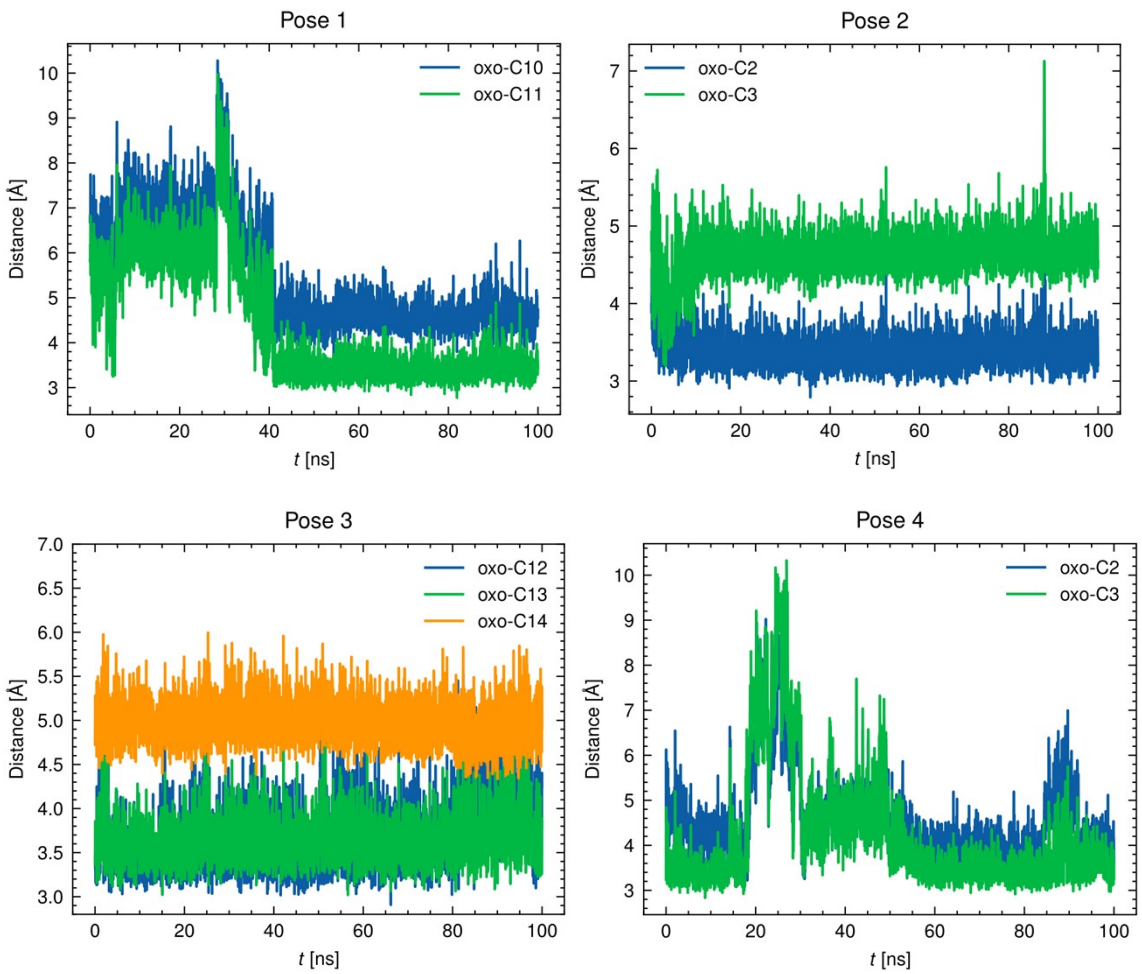

Figure S5: *Some distances discussed in the main text, during the 100 ns MD simulations of the substrate in different poses.*

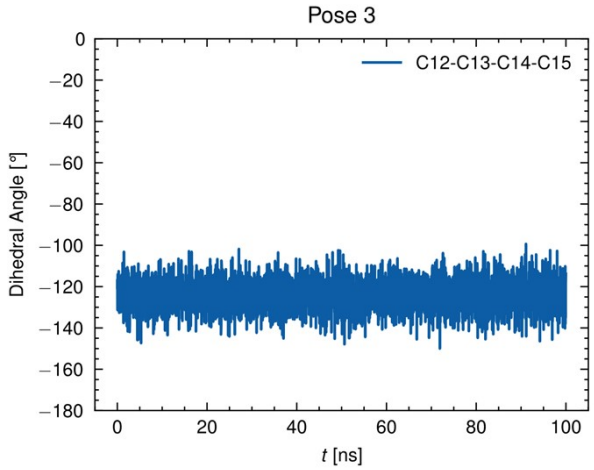

Figure S6: *Value of the C12-C13-C14-C15 dihedral angle of the substrate during the 100 ns MD simulation in pose 3.*

References

(1) Kim, V. C.; Kim, D. G.; Lee, S. G.; Lee, G. H.; Lee, S. A.; Kang, L. W. Crystal Structure of Cytochrome P450 184A1 from Streptomyces Avermitilis. **2023**.

(2) Wan, N.-W.; Cui, H.-B.; Zhao, L.; Shan, J.; Chen, K.; Wang, Z.-Q.; Zhou, X.-J.; Cui, B.-D.; Han, W.-Y.; Chen, Y.-Z. Directed Evolution of Cytochrome P450DA Hydroxylase Activity for Stereoselective Biohydroxylation. *Catal. Sci. Technol.* **2022**, *12* (18), 5703–5708. https://doi.org/10.1039/D2CY00164K.

(3) Keita, O.; Osami, S.; Yuichiro, A.; Hiroshi, S. Structure of the Manganese Protoporphyrin IX-Reconstituted CYP102A1 Heme Domain with N-Palmitoyl-L-Phenylalanine. **2023**.

(4) Ren, X. K.; Yorke, J. A.; Taylor, A.; Zhang, A. L.; Zhang, T.; Zhou, W. H.; Wong, L. -L. Expanding the Drug Metabolism Function of P450BM3. **2015**.

(5) Whitehouse, C. J. C.; Bell, S. G.; Yang, W.; Yorke, J. A.; Blanford, C. F.; Strong, A. J. F.; Morse, E. J.; Bartlam, M.; Rao, Z.; Wong, L.-L. A Highly Active Single-Mutation Variant of P450BM3 (CYP102A1). *ChemBioChem* **2009**, *10* (10), 1654–1656. https://doi.org/10.1002/cbic.200900279.

(6) Wan, N. W. Crystal Structure of Cytochrome P450DA Mutant (N190F/V356L/A486E) Heme Domain. **2021**.

(7) Fujiyama, K.; Hino, T.; Kanadani, M.; Watanabe, B.; Jae Lee, H.; Mizutani, M.; Nagano, S. Structural Insights into a Key Step of Brassinosteroid Biosynthesis and Its Inhibition. *Nat. Plants* **2019**, *5* (6), 589–594. https://doi.org/10.1038/s41477-019-0436-6.

(8) Kim, K.-H.; Lee, C. W.; Dangi, B.; Park, S.-H.; Park, H.; Oh, T.-J.; Lee, J. H. Crystal Structure and Functional Characterization of a Cytochrome P450 (BaCYP106A2) from Bacillus Sp. PAMC 23377. **2017**, *27* (8), 1472–1482. https://doi.org/10.4014/jmb.1706.06013.

(9) Janocha, S.; Carius, Y.; Hutter, M.; Lancaster, C. R. D.; Bernhardt, R. Crystal Structure of CYP106A2 in Substrate-Free and Substrate-Bound Form. *ChemBioChem* **2016**, *17* (9), 852–860. https://doi.org/10.1002/cbic.201500524.

(10) Zhang, B.; Lewis, K. M.; Abril, A.; Davydov, D. R.; Vermerris, W.; Sattler, S. E.; Kang, C. Structure and Function of the Cytochrome P450 Monooxygenase Cinnamate 4-Hydroxylase from Sorghum Bicolor 1. *Plant Physiol.* **2020**, *183* (3), 957–973. https://doi.org/10.1104/pp.20.00406.

(11) Herzog, K.; Bracco, P.; Onoda, A.; Hayashi, T.; Hoffmann, K.; Schallmey, A. Enzyme–Substrate Complex Structures of CYP154C5 Shed Light on Its Mode of Highly Selective Steroid Hydroxylation. *Acta Crystallogr. D Biol. Crystallogr.* **2014**, *70* (11), 2875–2889. https://doi.org/10.1107/S1399004714019129.

(12) Bracco, P.; Wijma, H. J.; Nicolai, B.; Buitrago, J. A. R.; Klünemann, T.; Vila, A.; Schrepfer, P.; Blankenfeldt, W.; Janssen, D. B.; Schallmey, A. CYP154C5 Regioselectivity in Steroid Hydroxylation Explored by Substrate Modifications and Protein Engineering**. *ChemBioChem* **2021**, *22* (6), 1099–1110. https://doi.org/10.1002/cbic.202000735.

(13) Abdulmughni, A.; Jóźwik, I. K.; Brill, E.; Hannemann, F.; Thunnissen, A.-M. W. H.; Bernhardt, R. Biochemical and Structural Characterization of CYP109A2, a Vitamin D3 25-Hydroxylase from Bacillus Megaterium. *FEBS J.* **2017**, *284* (22), 3881–3894. https://doi.org/10.1111/febs.14276.

(14) Debnath, A.; Calvet, C. M.; Jennings, G.; Zhou, W.; Aksenov, A.; Luth, M. R.; Abagyan, R.; Nes, W. D.; McKerrow, J. H.; Podust, L. M. CYP51 Is an Essential Drug Target for the Treatment of Primary Amoebic Meningoencephalitis (PAM). *PLoS Negl. Trop. Dis.* **2017**, *11* (12), e0006104. https://doi.org/10.1371/journal.pntd.0006104.

(15) Kim, K.-H.; Do, H.; Lee, C. W.; Subedi, P.; Choi, M.; Nam, Y.; Lee, J. H.; Oh, T.-J. Crystal Structure and Biochemical Analysis of a Cytochrome P450 Steroid Hydroxylase (BaCYP106A6) from Bacillus Species. **2023**, *33* (3), 387–397. https://doi.org/10.4014/jmb.2211.11031.

(16) Podust, L. M.; Jennings, G.; Calvet-Alvarez, C.; Debnath, A. Structure of the Naegleria Fowleri CYP51 at 1.7 Angstroms Resolution. **2017**.

(17) Wang, X.; Pan, H.; Sagurthi, S.; Paris, V.; Zhuo, C.; Dixon, R. A. The Protein Conformational Basis of Isoflavone Biosynthesis. *Commun. Biol.* **2022**, *5* (1), 1–10. https://doi.org/10.1038/s42003-022-04222-x.
(18) Dangi, B.; Lee, C. W.; Kim, K.-H.; Park, S.-H.; Yu, E.-J.; Jeong, C.-S.; Park, H.; Lee, J. H.; Oh, T.-J. Characterization of Two Steroid Hydroxylases from Different Streptomyces Spp. and Their Ligand-Bound and -Unbound Crystal Structures. *FEBS J.* **2019**, *286* (9), 1683–1699. https://doi.org/10.1111/febs.14729.
(19) Race, P. R.; Zulkepli, A. Z.; Anderson, R. J. L. Bacillus Subtilis 168 Bacillaene Polyketide Synthase (PKS) Cytochrome P450 PksS. **2016**.
(20) Carius, Y.; Hutter, M.; Kiss, F.; Bernhardt, R.; Lancaster, C. R. D. Structural Comparison of the Cytochrome P450 Enzymes CYP106A1 and CYP106A2 Provides Insight into Their Differences in Steroid Conversion. *FEBS Lett.* **2022**, *596* (24), 3133–3144. https://doi.org/10.1002/1873-3468.14502.